ISBN: 978-3-95450-184-7 doi:10.18429/JACoW-IPAC2018-WEPAF017

CORRECTION OF ID-INDUCED TRANSVERSE LINEAR COUPLING AT NSLS-II*

Y. Hidaka†, Y. Li, T. Shaftan, T. Tanabe, Y. Tian, G. Wang,
Brookhaven National Laboratory, Upton, NY 11973 USA

Abstract

Sizeable lifetime jumps have been observed sporadically since March 2016 at NSLS-II. These jumps were found to coincide with insertion device (ID) gap motions. Particularly, one of the in-vacuum undulators (IVUs) at Cell 17 was discovered to have large localized skew quadrupole component variation with gap. To allow the machine to operate stably in the low-emittance mode, a global coupling feedforward system has been recently implemented and successfully deployed. After installation of a new additional skew quadrupole, coupling compensation of this ID is now performed by a local coupling feedforward system. Furthermore, the maximum gap limit of all the existing IVUs has been decreased from 40 mm to 25 mm to limit the skew component variation during user operation.

INTRODUCTION

Stability of vertical beam size is one of the most important beam parameters to be maintained for synchrotron light source users [1,2], as it affects photon beam brightness if e-beam vertical emittance is not diffraction limited. Even though many third-generation light source facilities can operate in the vertically diffraction limited regime, operational vertical emittance could be set to a value larger than the diffraction limit in order to increase beam lifetime, as is done at NSLS-II (20-30 pm).

During user beam operation, ID gaps and phases are freely adjusted by beamline scientists. These state changes can introduce orbit distortion, tune change, and skew quadrupole errors, all of which can end up altering beam size due to coupling change.

At NSLS-II, an orbit feedforward system was always completed for every ID before beamline commissioning was started. However, coupling change due to skew quadrupole component variation with ID state changes has not been handled. This paper reports the recent results of our effort to minimize variation in vertical beam size (and emittance) and beam lifetime during ID gap motion.

ID-INDUCED COUPLING CHANGE

Large lifetime jumps during beamline operation have been occasionally observed since March 2016 at NSLS-II. Upon investigation, these events were found to be correlated with the gap motion of one of the IVUs called AMX at Cell 17. In a user operating condition, beam lifetime of 9.6 hr and vertical emittance of 17 pm at the minimum gap of 6.4 mm changed into 14.8 hr and 41 pm, respectively, after its gap was fully opened to 40 mm. Other IDs also caused changes in lifetime and vertical beam size (and emittance), but their impact was not nearly as much as that of AMX.

* Work supported by U.S. DOE under Contract No. DE-AC02-98CH10886.
† yhidaka@bnl.gov

MAGNETIC FIELD MEASUREMENTS

The integrated skew quadrupole component of AMX (C17-1) from a flip coil measurement [3] is shown in Fig. 1. For the full gap range, the change in skew quadrupole (SQ) strength is ~300 G. Other IVUs such as SRX (C05), LIX (C16) and FMX (C17-2) also have 150-250 G variation between their minimum and maximum gaps according to pre-installation magnetic field measurements. AMX is unique in that its Hall probe measurement at its minimum gap indicates strong SQ error locally concentrated at the ID entrance as shown in Fig. 2. The magic fingers at that location could be the cause of this error.

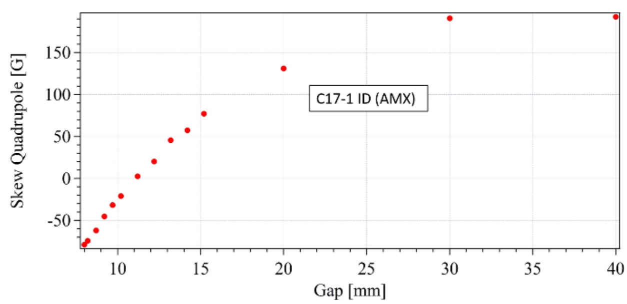

Figure 1: Integrated skew quad component (measured by flip coil) vs. gap for AMX.

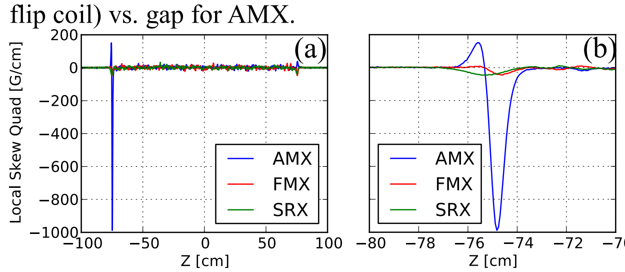

Figure 2: Local SQ strength for 3 different IVUs vs. z (longitudinal position) measured by Hall probe: (a) entire device length and (b) only near entrance.

BEAM-BASED COUPLING MEASUREMENTS & CORRECTIONS

The localization of strong SQ component at the entrance of AMX was also confirmed from measurements using e-beam. The strengths of SQ components at the IDs were estimated using DTBLOC [4], a recently developed linear optics/coupling characterization/correction tool based on resonance driving terms extracted from turn-by-turn (TbT) data. An example of SQ strength estimates for all the 15 ring SQ correctors and a virtual thin SQ element

Content from this work may be used under the terms of the CC BY 3.0 licence (© 2018). Any distribution of this work must maintain attribution to the author(s), title of the work, publisher, and DOI.

ISBN: 978-3-95450-184-7 doi:10.18429/JACoW-IPAC2018-WEPAF017

placed at the entrance of AMX is shown in Fig. 3. The TbT data for this was obtained after minimizing linear coupling with AMX gap fully open and then closing it to minimum. As expected, the SQ error estimate plot shows a spike only at the thin virtual element. Table 1 shows the estimated SQ strengths for the cases of having a thick (uniformly distributed) virtual SQ element, and a thin element at the entrance, center, and exit of 3 different IDs at their minimum gaps of 6.4 mm: AMX, FMX, and SRX. AMX fits better (i.e., larger χ^2 reduction factor) if a thin error source at entrance is assumed, which is consistent with the Hall probe measurement. FMX and SRX appear to have no strong localized error, as χ^2 reduction factors do not differ much among these different assumptions.

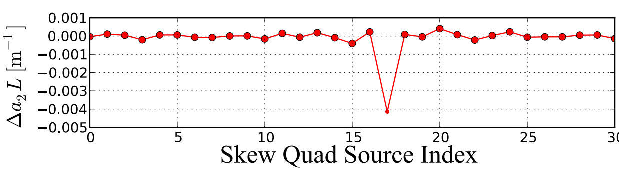

Figure 3: Integrated SQ strength errors around the ring when AMX is closed to the minimum gap of 6.4 mm.

Table 1: Integrated SQ Strength Estimates for AMX, FMX, & SRX with Different Error Source Assumptions

	Integrated SQ [G]	**χ^2 Reduction Factor**
AMX: Thin @ Entrance	-578.3	101.1
AMX: Thin @ Center	-958.1	80.7
AMX: Thin @ Exit	-1529.2	50.7
AMX: Thick (1.5 m)	-974.6	61.8
FMX: Thin @ Entrance	-304.5	16.4
FMX: Thin @ Center	-197.8	17.8
FMX: Thin @ Exit	-118.6	17.6
FMX: Thick (1.5 m)	-171.6	17.3
SRX: Thin @ Entrance	-76.6	25.5
SRX: Thin @ Center	-48.9	25.7
SRX: Thin @ Exit	-29.4	25.7
SRX: Thick (1.5 m)	-44.4	25.7

SHORT-TERM SOLUTION

A global coupling feedforward system was first implemented to minimize the impact of the ID-induced SQ errors to allow stable operation in low-emittance mode. The existing 15 ring SQs were used by this system. The corrections only for AMX were included, but can be easily expanded to include the other IDs.

It took only 25 minutes for data acquisition and another 25 minutes to process the data to generate a feedforward table at 12 different gap values of AMX using the same coupling correction tool used in the previous section. One iteration was sufficient. Figure 4 shows how effective this table was in a nominal user operation condition: The vertical emittance (beam size) change of 260% (60%) and the beam current lifetime product change of 53% without the feedforward system was reduced to 8% (4%) and 11%, respectively. The table was generated at a low current of 2 mA, but was equally effective at a high current of 250mA.

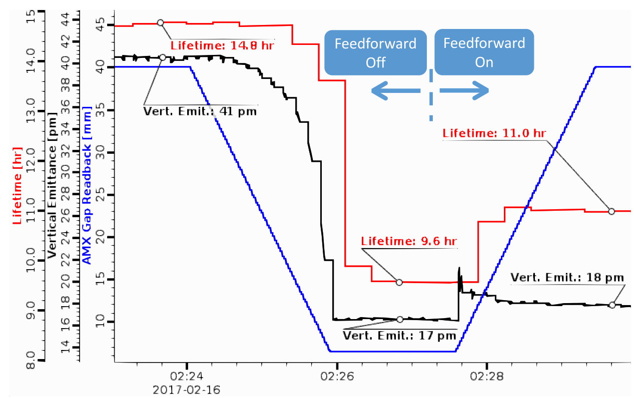

Figure 4: Effectiveness of global coupling correction for AMX SQ strength variation with gap.

LONG-TERM SOLUTIONS

Although the global feedforward system was effective, it was only a temporary solution. As a more permanent solution, we considered re-shimming of AMX to reduce the SQ error, but deemed too costly.

We also considered swapping of the IVUs installed on the same straight section due to resonance driving term (RDT) analysis. The RDTs for linear coupling, f_{1001} and f_{1010}, can be expressed as follows [1]:

$$f_{\substack{1001\\1010}}(s) \approx \frac{\sum_w (\Delta a_2 L)_w \sqrt{\beta_{x,w}\beta_{y,w}} \cdot e^{i\left(\Delta\phi_x^{w,s} \mp \Delta\phi_y^{w,s}\right)}}{4\left(1-e^{i\cdot 2\pi(\nu_x \mp \nu_y)}\right)}, \quad (1)$$

with $\Delta a_2 L$ as the integrated field strengths of SQs, ν_x and ν_y as horizontal and vertical tunes, $\beta_{x,w}$ and $\beta_{y,w}$ as horizontal and vertical beta functions at the SQs, and $\phi_x^{w,s}$ and $\phi_y^{w,s}$ as the horizontal and vertical phase advances between locations of the observations and the SQs. Note all the Twiss parameters are those for an uncoupled lattice. Cell 17 straight is a canted straight with identical IVUs, AMX (upstream) and FMX (downstream), symmetrically installed around the center of the straight. Because $\sqrt{\beta_{x,w}\beta_{y,w}}$ is 2.7 times larger at entrance than at exit for AMX, and vice versa for FMX, swapping the two would have reduced coupling impact by ~60%. Even though this reduction is significant, residual error is still large. Hence, this solution was not adopted, either.

One remedy we actually put in place for the IDs themselves was the modification of the maximum gaps of all the IVUs. Originally the max gap was set to 40 mm, but they have been reduced to 25 mm to limit the SQ variation over the full gap range. This change was also better in terms of impedance, due to less discontinuity in vacuum pipe height.

The main permanent solution for the large SQ variation for AMX, however, was implementation of a local coupling feedforward system with installation of a new dedicated SQ. As evident from Eq. (1), strictly speaking, four SQs are needed to correct one SQ error source, as there

Content from this work may be used under the terms of the CC BY 3.0 licence (© 2018). Any distribution of this work must maintain attribution to the author(s), title of the work, publisher, and DOI.

ISBN: 978-3-95450-184-7 doi:10.18429/JACoW-IPAC2018-WEPAF017

Content from this work may be used under the terms of the CC BY 3.0 licence (© 2018). Any distribution of this work must maintain attribution to the author(s), title of the work, publisher, and DOI.

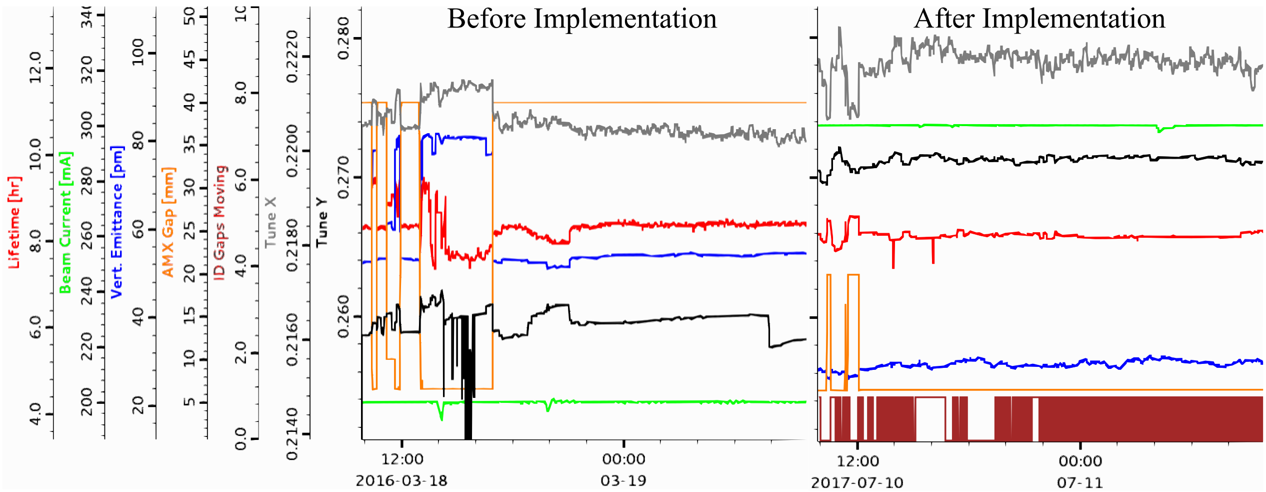

Figure 6: Comparison of 24-hr history data for beam size, lifetime, and ID gap motions before and after implementation of local coupling feedforward system.

are 2 complex RDT values to be compensated. However, due to our choice of fractional tunes (0.22, 0.26), the difference RDT f_{1001} dominates over the sum RDT f_{1010}. Therefore, 2 SQs placed at different phases are sufficient to correct most of coupling error. Moreover, if placed at a right location, even one SQ can cancel majority of coupling error. If the f_{1001} phase at the correction SQ is within 10° (or near 180°) from the f_{1001} phase at the ID SQ

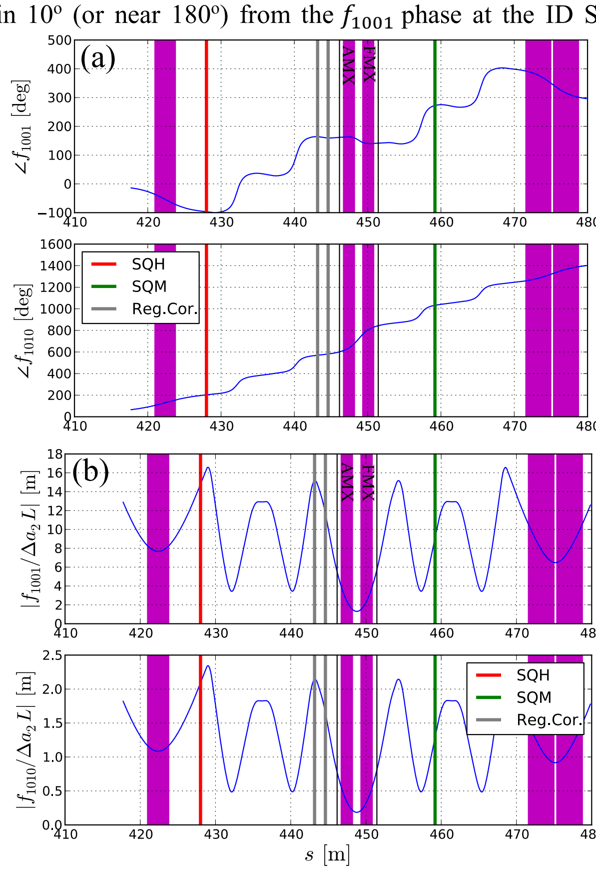

Figure 5: Variation of linear coupling RDT phase and magnitude around C17 to search for a new SQ candidate location.

error source, good coupling correction is possible. As shown in Fig. 5, an existing slow orbit corrector (C16-CL1) immediately upstream of AMX (grey strip at $s \sim$ 443 m) turned out to be the best location. This magnet was converted to a combined orbit/SQ corrector during 2017 Spring Shutdown. After installation, a new coupling feedforward table was generated using just this new SQ with the same method. The resulting effectiveness of this local coupling feedforward system is shown in Table 2. Figure 6 compares 24-hr history data of various beam/machine states such as beam lifetime, vertical beam size and the ID states before implementation of the local coupling feedforward system. Significant improvement in beam size stability is clearly seen.

Table 2: Effectiveness of Local Coupling Feedforward System for AMX at Nominal Operating Condition (Total Beam Current of 300 mA with all IDs at Nominal Gaps)

Gap [mm]	τ [hr] FF Off	τ [hr] FF On	σ_y [μm] FF Off	σ_y [μm] FF On
25	11.2	11.2	30.3	30.3
7.0	9.3 (-17.0%)	11.1 (-0.9%)	26.2 (-13.5%)	31.2 (+3.0%)
6.4	8.5 (-24.1%)	10.7 (-4.5%)	25.0 (-17.5%)	30.9 (+2.0%)

CONCLUSION

We have observed coupling errors larger than expected when ID gaps are changed at NSLS-II. We have resolved this issue by first implementing a global coupling feedforward system utilizing only the existing hardware. Later a new skew quadrupole was strategically introduced to locally contain the coupling error induced by the most offensive ID. The new local coupling feedforward system has been successfully commissioned and in operation since June 2017.

ISBN: 978-3-95450-184-7 doi:10.18429/JACoW-IPAC2018-WEPAF017

REFERENCES

[1] A. Franchi, L. Farvacque, J. Chavanne, F. Ewald, B. Nash, K. Scheidt, and R. Tomas, "Vertical emittance reduction and preservation in electron storage rings via resonance driving terms correction", in *Phys. Rev. ST Accel. Beams*, vol. 14, p. 034002 (2011).

[2] C. Steier, "Coupling Control and Optimization in DLSRs," High-Brightness Synchrotron Light Source Workshop, Upton, NY, USA (2017). https://indico.bnl.gov/event/2938/contributions/7793/attachments/6995/8567/019_Steier_Coupling_Control_and_Optimization.pdf

[3] T. Tanabe, C. Kitegi, P. He, M. Musardo, D. Hidas, J. Rank *et al.*, "Latest Experience on Insertion Devices at the National Synchrotron Light Source-II", in *Journal of the Vacuum Society of Japan* Vol. 59, No.8 (2016).

[4] Y. Hidaka, B. Podobedov, and J. Bengtsson, "Linear Optics Characterization and Correction Method using Turn-by-Turn BPM Data Based on Resonance Driving Terms with Simultaneous BPM Calibration Capability," in *Proc. NAPAC'16*, Chicago, IL, USA (2016), TUPOB52.

Content from this work may be used under the terms of the CC BY 3.0 licence (© 2018). Any distribution of this work must maintain attribution to the author(s), title of the work, publisher, and DOI.